A Direct Imaging Method Using Far Field Data *

Songming Hou † Knut Solna ‡ Hongkai Zhao‡

January 9, 2007

Abstract

We present a direct imaging algorithm for extended targets using far field data generated by incident plane waves. The algorithm uses a factorization of the response matrix for far field data that derives from physical considerations, moreover, a resolution based regularization. The algorithm is simple and efficient since no forward solver or iteration is needed. Efficiency and robustness of the algorithm with respect to measurement noise are demonstrated.

Keywords: far field, singular value decomposition, response matrix, MUSIC.

1 Introduction

Probing a medium using incident plane waves and recording far field pattern is a classical inverse scattering problem that has been studied in depth. The objective is to find the location and geometry of the targets using the far field pattern of the scattering operator, that is, using the relation between incident plane waves and scattered outgoing plane waves.

There are essentially two type of methods that have been presented to solve such an inverse problem: iterative methods and direct methods. Iterative methods treat the inverse problem as a nonlinear optimization problem. Usually, for each iteration, an adjoint forward problem needs to be solved. Direct method gives a characterization/visualization of the geometry by designing an imaging function that peaks near the target boundary.

For example, the MUltiple SIgnal Classification (MUSIC) algorithm [6, 8, 10, 14, 15] is a direct imaging function which can locate small targets using an array of transducers that can send and receive signals. The MUSIC algorithm is generalized in [9] to image the shape of extended targets for near field data. In this paper, we generalize the MUSIC algorithm to solve the inverse scattering problem for far field data. This method is a direct method that is very efficient and robust. It can be parallelized easily since the evaluation at different search points are independent.

The linear sampling method, first proposed in [4], is also a direct imaging algorithm for the inverse scattering problem. The method is based on a characterization of the range of the scattering operator for the far field pattern. It is shown that the far field pattern of a point source located inside the object is in the range of the scattering operator. Kirsch presents a factorization of the scattering operator in [11] and uses this factorization for imaging. The relation between the MUSIC and the linear sampling method is studied in [2, 12]. A good

*The research is partially supported by ONR grant N00014-02-1-0090, DARPA grant N00014-02-1-0603, NSF grant 0307011 and the Sloan Foundation.

†Dept of Math, Michigan State Univ., East Lansing, MI, 48824, mickey@math.msu.edu

‡Dept of Math, Univ. of Cal. at Irvine, CA, 92697. ksolna, zhao@math.uci.edu

review of the recent development of the linear sampling method is presented in [1, 3]. As in the case of the linear sampling method our approach is based on a frequency domain formulation. The approach presented here differ from the linear sampling method. First, our algorithm is based on a different factorization. Second, a resolution based thresholding is used for regularization, which is very robust with respect to noise.

The outline of the paper is as follows. In Section 2, we briefly explain the original MUSIC algorithm and apply it to far field data to find the locations of small targets, that is, the data we use is low frequency data so that the target size is much smaller than wave length. In Section 3, we formulate the generalized MUSIC algorithm for far field data. Then, in Section 4, we discuss the generalized MUSIC imaging function for sound-hard targets. Finally, we provide numerical experiments in Section 5 to demonstrate the efficiency and robustness of our imaging algorithm.

2 Imaging the Location of Point Targets.

In this section we generalize the basic MUSIC algorithm to the case with small targets in a situation with far field data. We shall analyze the situation with a general non-symmetric response matrix and define next the multi-static response matrix for far field data in the frequency domain. Consider an array of transducers that can send out plane incident (probing) waves and record outgoing (scattered) plane waves in various directions (angles). Assume that we have a set of incident plane waves with incident angles (directions) $\hat{\alpha}_i, i = 1, \ldots, m$. The scattered waves are recorded at outgoing angles $\hat{\beta}_j, j = 1, \ldots, n$. Here $\hat{\alpha}_i, \hat{\beta}_j$ belong to the unit sphere $S^d, d = 2, 3$, These measurements form the m-by-n response matrix P. The response matrix can be regarded as a discrete version of the scattering operator. Also we define the physical resolution of the array in the same way as in [6] and [9]: Consider the far field signal generated by a point source that is time reversed (phase conjugated in the frequency domain) and sent back, the focusing size of the resent signal is the physical resolution of the array. The resolution is related to the wavelength and the aperture of the array. If the array has full aperture so that the full angular variation is resolved, then the resolution of the array is the wavelength. In general the physical resolution of an array can be determined using physical experiments or multiple frequency data [9].

If the dimensions of the targets are much smaller than the physical resolution of the array then the targets can be regarded as point scatterers. The structure of the response matrix is then greatly simplified since the geometry and material properties of the targets are neglected. The following formulation is similar to that in [12], it is more general in that the incoming and outgoing directions may be different.

Assume that there are M point targets located at $\mathbf{y}_1, \ldots, \mathbf{y}_M \in R^d, d = 2, 3$. For an incident plane wave coming in the direction $\hat{\theta} \in S^d$,

$$u^i(\mathbf{x}, \hat{\theta}) = \mathbf{e}^{\mathbf{ikx}\cdot\hat{\theta}},$$

where k is the wave number, the scattered wave field is

$$u^s(\mathbf{x}, \hat{\theta}) = \sum_{l=1}^{M} \tau_l e^{ik\mathbf{y}_l\cdot\hat{\theta}} G(\mathbf{x}, \mathbf{y_l}),$$

if multiple scattering among point targets are neglected. Here $G(\mathbf{x}, \mathbf{y})$ is the Green function for the Helmholtz equation which has the far field pattern

$$G(\mathbf{x}, \mathbf{y}) = \gamma_{\mathbf{d}} \frac{\mathbf{e}^{\mathbf{ik}\|\mathbf{x}\|}}{\|\mathbf{x}\|^{(\mathbf{d-1})/\mathbf{2}}} \mathbf{e}^{-\mathbf{ik}\hat{\mathbf{x}}\cdot\mathbf{y}} + \mathbf{O}(\|\mathbf{x}\|^{-(\mathbf{d+1})/\mathbf{2}}), \qquad \|\mathbf{x}\| \to \infty.$$

where

$$\hat{\mathbf{x}} = \frac{\mathbf{x}}{\|\mathbf{x}\|}, \quad \gamma_2 = \frac{1+i}{4\sqrt{k\pi}}, \quad \gamma_3 = \frac{1}{4\pi}.$$

The far field pattern of the scattered field is accordingly defined by

$$u_\infty(\hat{\mathbf{x}}, \hat{\theta}) = \sum_{l=1}^{M} \tau_l e^{ik\mathbf{y}_l \cdot (\hat{\theta} - \hat{\mathbf{x}})},$$

so that the elements of the response matrix are

$$P_{ij} = u_\infty(\hat{\beta}_j, \hat{\alpha}_i) = \sum_{l=1}^{M} \tau_l e^{ik\mathbf{y}_l \cdot (\hat{\alpha}_i - \hat{\beta}_j)}.$$

The response matrix can therefore be decomposed in the form

$$P = \sum_{l=1}^{M} \hat{\mathbf{g}}_l^i [\hat{\mathbf{g}}_l^o]^H,$$

where H denotes the Hermitian. If we assume $M < \min(m, n)$ the response matrix P is of rank M. The column space is spanned by the following illumination vectors with respect to the incident wave directions

$$\hat{\mathbf{g}}_l^i = [e^{ik\hat{\alpha}_1 \cdot \mathbf{y}_l}, \ldots, e^{ik\hat{\alpha}_m \cdot \mathbf{y}_l}]^T, \quad l = 1, 2, \ldots, M.$$

The row space is spanned by the following illumination vectors with respect to the outgoing wave directions

$$\hat{\mathbf{g}}_l^o = [e^{ik\hat{\beta}_1 \cdot \mathbf{y}_l}, \ldots, e^{ik\hat{\beta}_n \cdot \mathbf{y}_l}]^T \quad l = 1, 2, \ldots, M,$$

with T denoting the transpose.

Now we define our imaging function which is similar to the original MUSIC algorithm and is based on the Singular Value Decomposition of the response matrix. We can either use the first M left singular vectors $\mathbf{u}_l$, $l = 1, 2, \ldots, M$

$$I_L(\mathbf{x}) = \frac{1}{1 - \sum_{l=1}^{M} |\hat{\mathbf{g}}_0^i(\mathbf{x}) \cdot \mathbf{u_l}|^{\mathbf{2}}}, \tag{1}$$

or use the first M right singular vectors $\mathbf{v}_l$, $l = 1, 2, \ldots, M$

$$I_R(\mathbf{x}) = \frac{1}{1 - \sum_{l=1}^{M} |\hat{\mathbf{g}}_0^o(\mathbf{x}) \cdot \mathbf{v_l}|^{\mathbf{2}}}, \tag{2}$$

or combine both. Here $\hat{\mathbf{g}}_0^i(\mathbf{x})$ and $\hat{\mathbf{g}}_0^o(\mathbf{x})$ are normalized illumination vectors at $\mathbf{x}$ with respect to the incoming and outgoing directions respectively. From the above analysis of the response matrix the imaging function will peak at the locations of the point targets.

Remark 1: The essential difference between the above algorithm and the original MUSIC is the use of the far field pattern of the Green function in the illumination vector. Note also that if the incoming and outgoing directions are the same the above two imaging functions become the same.

Remark 2: The above imaging function will also work in the case with multiple scattering among point targets. It is shown in [8] that the column and row spaces are not changed by multiple scattering using the Foldy-Lax formula.

3 Imaging Extended Target

We next discuss the properties of the Singular Value Decomposition of the response matrix in the general case. In general the singular value decomposition of the response matrix can have the following three patterns.

For point targets whose sizes are much smaller than the array resolution, the number of significant singular values equals to the number of targets and the response matrix only contains location information.

For small targets whose sizes are smaller than, but comparable to the array resolution, the pattern of singular values becomes more complicated as explained in [16]. The response matrix contains location and some size information.

For extended targets whose sizes are larger than the array resolution, the response matrix contains both location and geometry information of the target. In [9] a direct imaging algorithm is developed for extended target. The key idea in the imaging algorithm is to determine

1. The illumination vector based on a physical factorization of the scattered field.

2. The signal space and its dimension (thresholding) based on a resolution analysis.

In the following we will show the proper form of illumination vector for far field data, that is, when using plane wave data. Let us first deal with sound soft targets with Dirichlet boundary condition at the target boundary. For simplicity we assume here that the outgoing directions we measure are the same as the incoming directions, $\hat{\theta}_1, \ldots, \hat{\theta}_n$. The scattered far field is then [5]

$$u_\infty(\hat{x}) = -\frac{1}{4\pi} \int_{\partial D} \frac{\partial u}{\partial \nu}(y) e^{-ik\hat{x}\cdot y} ds(y), \tag{3}$$

where ∂D is the boundary of the targets, $\hat{x}$ is a unit vector that defines the far field direction, u is the total field, ν is the outer normal direction on the boundary of the targets. The constant $-\frac{1}{4\pi}$ corresponds to 3-dimensional problems and it is replaced by $-\frac{e^{i\pi/4}}{\sqrt{8\pi|k|}}$ for 2-dimensional problems. In our setup, the element of the response matrix P_{ij} corresponds to the far field pattern of the scattered field in the jth direction due an incident wave coming from the ith direction, e.g.,

$$P_{ij} = u_\infty(\hat{\theta_j}; \hat{\theta_i}) = -\frac{1}{4\pi} \int_{\partial D} \frac{\partial u}{\partial \nu}(y; \hat{\theta}_i) e^{-ik\hat{\theta}_j \cdot y} ds(y),$$

where the total field is due to incident plane wave coming from the direction $\hat{\theta}_i$. In the matrix form

$$P = -\frac{1}{4\pi} \int_{\partial D} \frac{\partial \vec{u}}{\partial \nu} \hat{\mathbf{g}}^T(y) ds(y), \tag{4}$$

where

$$\hat{\mathbf{g}}(y) = [e^{-ik\hat{\theta}_1 \cdot y}, \ldots, e^{-ik\hat{\theta}_n \cdot y}]^T, \tag{5}$$

and $\vec{u}$ is the vector of total fields corresponding to the incident plane waves from $\hat{\theta}_1, \ldots, \hat{\theta}_n$. Equation (4) gives a physical factorization of the scattered field into known and unknown parts. The far field pattern is a superposition of the far field patterns of point sources located on the boundary of the target, however, we do not know the weight function which depends

on the total field. In other words, the scattering at the target boundary acts as sources for the scattered field. In this far field setup, it is natural to use $\hat{\mathbf{g}}(y)$ as the illumination vector. The signal space of the response matrix should be well approximated by the span of the illumination vectors $\hat{\mathbf{g}}(y)$ with y on the well-illuminated part of the boundary of the targets.

The next step is to determine the signal space, which is spanned by appropriate leading singular vectors of the response matrix. It has been shown in [9] that by using a resolution analysis based thresholding, we could determine a threshold r and use the first r singular vectors to image the shape of the targets. This procedure is the same for far field data. The thresholding for a special case with circular shape target for far field data is discussed in [7].

Let $\mathbf{v}_1, \ldots, \mathbf{v}_r$ be the first r leading singular vectors for the response matrix, the MUSIC imaging function for far field data can be defined using the illumination vectors for far field data given in (5).

$$I(\mathbf{x}) = \frac{\mathbf{1}}{\mathbf{1} - \sum_{\mathbf{j=1}}^{\mathbf{r}} \mid \hat{\mathbf{g}}_{\mathbf{0}}(\mathbf{x}) \cdot \mathbf{v_j} \mid^{\mathbf{2}}} \tag{6}$$

where $\hat{\mathbf{g}}_0$ is the normalized illumination vector.

We could combine the imaging functions for different frequencies to improve robustness of the result. The multiple-frequency MUSIC imaging function reads:

$$I(\mathbf{x}) = \frac{\mathbf{1}}{\mathbf{m} - \sum_{\mathbf{q=1}}^{\mathbf{m}} \sum_{\mathbf{j=1}}^{\mathbf{r_q}} \mid \hat{\mathbf{g}}_{\mathbf{0}}^{\mathbf{q}}(\mathbf{x}) \cdot \mathbf{v}_{\mathbf{j}}^{\mathbf{q}} \mid^{\mathbf{2}}} \tag{7}$$

where m is the number of frequencies used.

Remark 3: If the set of incident angles coincide with the set of outgoing angles the response matrix is symmetric due to reciprocity. Otherwise the column signal space of the response matrix is spanned by the illumination vectors corresponding to the incident angles and the row signal space is spanned by illumination vectors corresponding to the outgoing angles. In this case both spaces can be used in imaging. See [9] for a more detailed discussion.

4 Neumann boundary condition

For a sound-hard target, the far field pattern of the scattered field is

$$u_\infty(\hat{x}) = -\frac{1}{4\pi} \int_{\partial D} u(y) \frac{\partial e^{-ik\hat{x}\cdot y}}{\partial \nu(y)} ds(y), \tag{8}$$

where u is the total field induced by an incident wave. So the response matrix is of the form

$$P = -\frac{1}{4\pi} \int_{\partial D} \vec{u}(y) \frac{\partial \hat{\mathbf{g}}^T(y)}{\partial \nu(y)} ds(y). \tag{9}$$

This shows that the signal space of the response matrix P should be well approximated by illumination vectors of the form $\frac{\partial \hat{\mathbf{g}}(y)}{\partial \nu(y)}$ with y being well-illuminated points on the boundary of the targets. However, the normal direction ν of the boundary is not known. Therefore, we use the same strategy as in [9] and incorporate a directional search among a few fixed directions in our imaging function.

The MUSIC imaging function is:

$$I(\mathbf{x}) = \frac{\mathbf{1}}{\mathbf{1} - \mathbf{max_j} \sum_{\mathbf{i=1}}^{\mathbf{r}} \mid \frac{\partial \hat{\mathbf{g}}_{\mathbf{0}}(\mathbf{x})^{\mathbf{H}}}{\partial \nu_{\mathbf{j}}} \mathbf{v_i} \mid^{\mathbf{2}}}, \tag{10}$$

where ν_j is a search direction for the normal direction and $\frac{\partial \tilde{\mathbf{g}}_0}{\partial \nu_j}$ is the normalized illumination vector for sound-hard targets. By taking the maximum over a few fixed directions we are able to find the correct normal direction on the boundary and use it for imaging. Again we can combine the imaging functions for different frequencies to improve robustness of the result. The corresponding multiple frequency MUSIC imaging function is:

$$I(\mathbf{x}) = \frac{\mathbf{1}}{\mathbf{m} - \sum_{\mathbf{q=1}}^{\mathbf{m}} \mathbf{max_j} \sum_{\mathbf{i=1}}^{\mathbf{r^q}} \mid \frac{\partial \tilde{\mathbf{g}}_{\mathbf{0}}^{\mathbf{q}}(\mathbf{x})^{\mathbf{H}}}{\partial \nu_{\mathbf{j}}} \mathbf{u}_{\mathbf{i}}^{\mathbf{q}} \mid^{\mathbf{2}}}. \tag{11}$$

Remark 4. If we use the MUSIC imaging function for sound-soft targets to image sound-hard targets, we will observe double-edge images, e.g., using two layers of monopole to approximate one layer of dipole, and vice versa. This issue is discussed in [9].

5 Numerical Experiments

We present some numerical examples to illustrate how our direct imaging method is capable of imaging sound-soft and sound-hard targets and its robustness with respect to noise. The multiplicative noise is modeled as follows:

$P_{new}(i,j) = real(P(i,j)) \cdot a_{ij} + imag(P(i,j)) \cdot b_{ij}$, where a_{ij}, b_{ij} are independent random numbers uniformly distributed in $[1-c, 1+c]$, where c is 100% in all our experiments. This corresponds to a signal-to-noise ratio of approximately 3. (NB HOW is SNR computed)

We implemented the method in [5] to generate the far field data $P(i,j)$ for sound-soft targets and the method in [13] to generate the data for the far field data $P(i,j)$ for sound-hard targets.

In all images we use the grid size $h = 0.1$ and the search domain is chosen to be a 100-by-100 sub-grid.

Consider a kite-shape sound-soft target and a circular shape sound-soft target. The size of each target is about 2. The separation distance between the targets is about 3. We use the wave number $k = 0.5$, that is, a wavelength of $2\pi/0.5$, much larger than the size of the targets. We use 32 incident plane waves and 32 far-field directions with equal angles to generate the response matrix. Moreover, we use the Nordström's method [5] to generate our forward data and corrupt the data with multiplicative noise corresponding to a signal-to-noise ratio of approximately 3 as explained above. Figure 1 and 2 show the singular value plot of the response matrix with and without the noise. Since the size of the targets are much smaller than the wavelength, there are two dominant singular values in each of the plots, corresponding to the two targets. Note that the noise perturbs the singular values but does not change the pattern significantly. Figure 3 shows the MUSIC imaging function (1) with $M = 2$. The location of the two targets are found. However, there is no shape information in the response matrix.

Next we consider the same setup as above but use $k = 7$. This time the wavelength $2\pi/7$ is smaller than the size of the targets. Therefore, the targets can be considered to be extended targets and the shape information is included in the response matrix. Figure 4 and 5 show the singular value plot of the response matrix with and without the noise. Since the sizes of the targets are larger than the wavelength, a "continuous" spectrum is observed. Again the noise perturbs the singular values but does not change the pattern significantly. Figure 6 shows the MUSIC imaging function (6) with $r = 14$, which is estimated by the resolution analysis based thresholding in [9]. We clearly see the kite and circular shapes even with the multiplicative noise.

Now we consider the same setup with a kite and a circle but use sound-hard targets. Figure 7 shows the MUSIC imaging function (7) for sound-hard targets.

Next, we show how multiple frequency data can help to improve the imaging. We now combine the imaging functions for $k = 5, 6, 7$ for the sound-soft targets and sound-hard targets. Figure 8 and 9 show the improved imaging functions (10) and (11) for sound-soft and sound-hard targets.

Finally, we illustrate the case with two targets that are very close to each other. Figure 10 shows the imaging function 6) with $k = 5$ and $r = 10$. The separation distance between the kite-shape and circular shape targets is about 0.5 and smaller than half the wave length. In this case the objects cannot be clearly separated.

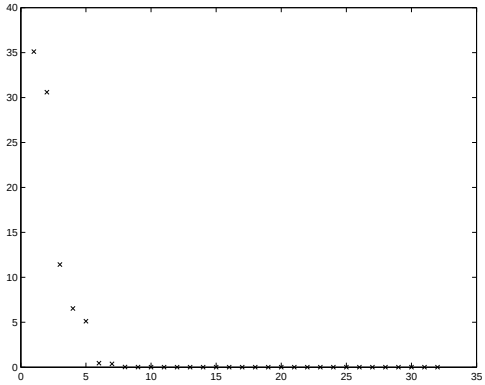

Figure 1: The singular value plot for the response matrix with $k = 0.5$ (size of the two targets much smaller than wavelength) for clean data, two dominant singular values are observed.

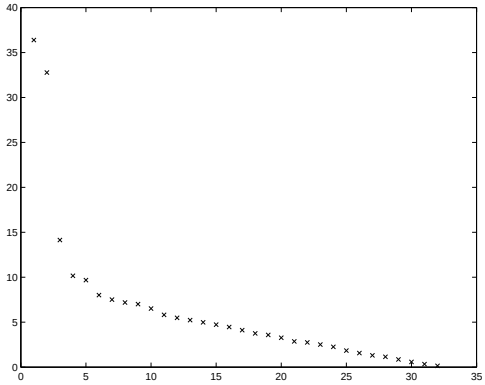

Figure 2: The singular value plot for the response matrix with $k = 0.5$ (size of the two targets much smaller than wavelength) for data with noise, two dominant singular values are observed.

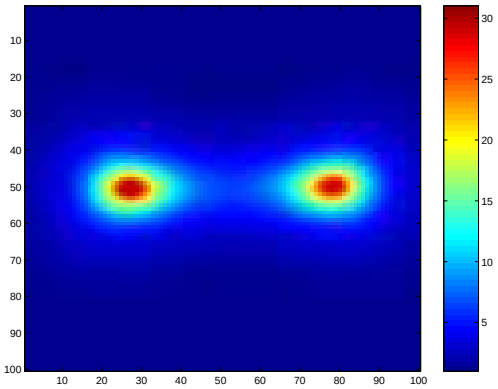

Figure 3: MUSIC imaging function with $k = 0.5$ for data with noise, the locations for the kite-shape and circular-shape sound-soft targets are found but no shape information.

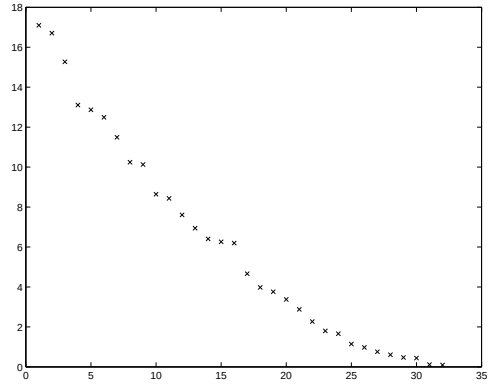

Figure 4: The singular value plot for the response matrix with $k = 7$ (size of the two targets larger than wavelength) for clean data, a "continuous" spectrum is observed.

6 Conclusions

We propose a direct imaging algorithm for farfield data based on a physical factorization of the scattering operator. The algorithm is simple and efficient because no forward solver or iteration is needed. Physical resolution based thresholding is used for regularization, which is robust with respect to measurement noise. The algorithm can also deal with different material properties and different type of illuminations and measurements. Furthermore, parallelization can be applied naturally since the evaluation at different search points are independent.

7 Acknowledgement

We would like to thank Russel Luke for helpful discussions on far field data.

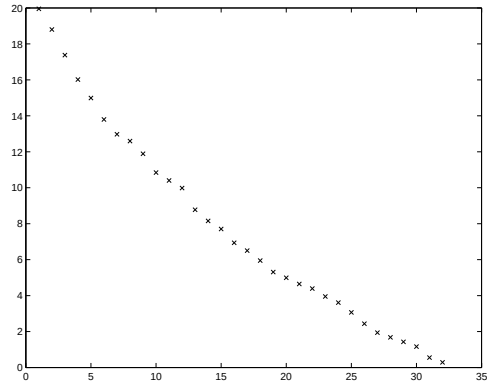

Figure 5: The singular value plot for the response matrix with $k = 7$ (size of the two targets larger than wavelength) for data with noise, a "continuous" spectrum observed.

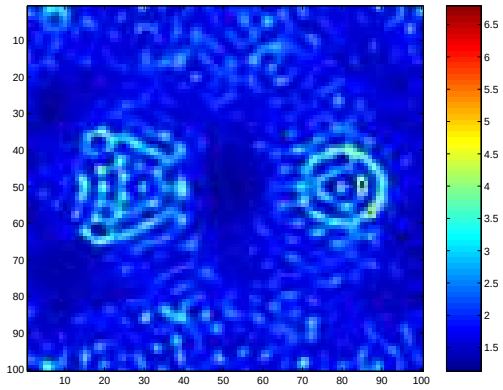

Figure 6: MUSIC imaging function with $k = 7$ for data with noise, the shape for the kite and circle for sound-soft targets are reconstructed.

References

[1] F. Cakoni and D. Colton. Qualitative methods in inverse scattering theory: An introduction. *Springer, Berlin*, 2005.

[2] M. Cheney. The linear sampling method and the music algorithm. *Inverse Problems*, 17:591–595, 2001.

[3] D. Colton, J. Coyle, and P. Monk. Recent developments in inverse acoustic scattering theory. *SIREV*, 42:369–414, 2000.

[4] D. Colton and A. Kirsch. A simple method for solving inverse scattering problems in the resonance region. *Inverse Problems*, 12:383–393, 1996.

[5] D. Colton and R. Kress. Inverse acoustic and electromagnetic scattering theory, 2nd edition. *Springer, Berlin*, 1998.

[6] A. J. Devaney. Super-resolution processing of multi-static data using time-reversal and MUSIC. *to appear in Journal of the Acoustical Society of America*.

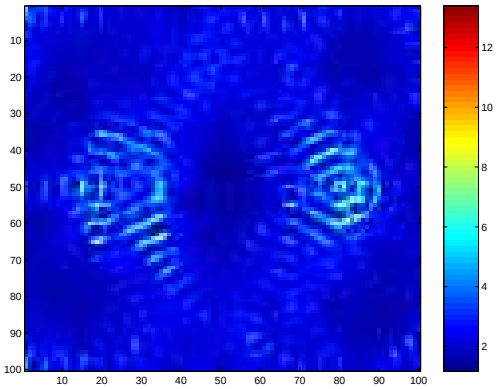

Figure 7: MUSIC imaging function with $k = 7$ for data with noise, the shape for the kite and circle for sound-hard targets are reconstructed.

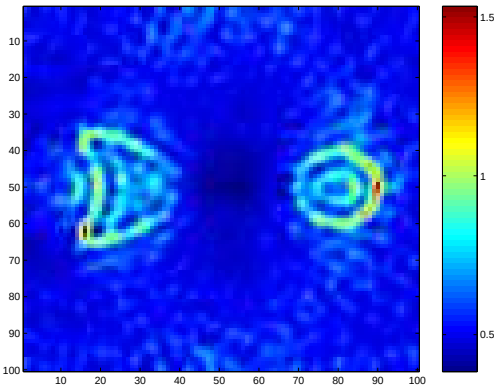

Figure 8: Multiple-frequency MUSIC imaging function with $k = 5, 6, 7$ for data with noise, the shape for the kite and circle for sound-soft targets are reconstructed. The image is clearer than the single frequency reconstruction.

[7] A. J. Devaney and R. Luke. Determining the shape of an object from scattered field data. *Preprint*, 2006.

[8] F. K. Gruber, E. A. Marengo, and A. J. Devaney. Time-reversal imaging with multiple signal classification considering multiple scattering between the targets. *J. Acoust. Soc. Am.*, 115:3042–3047, 2004.

[9] S. Hou, Knut Solna, and Hongkai Zhao. A direct imaging algorithm for extended targets. *Inverse Problems*, 22:1151–1178, 2006.

[10] E. Kerbrat, C. Prada, and M. Fink. Imaging in the presence of grain noise using the decomposition of the time reversal operator. *Journal of the Acoustical Society of America*, 113(3):1230–1240, March 2003.

[11] A. Kirsch. Charactorization of the shape of a scattering obstacle using the spactral data of the far-field operator. *Inverse Problems*, 14:1489–1512, 1998.

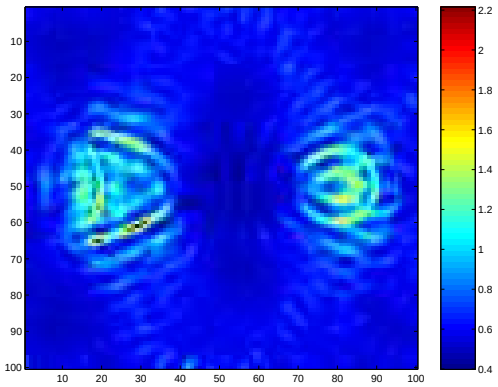

Figure 9: Multiple-frequency MUSIC imaging function with $k = 5, 6, 7$ for data with noise, the shape for the kite and circle for sound-hard targets are reconstructed. The image is clearer than the single frequency reconstruction.

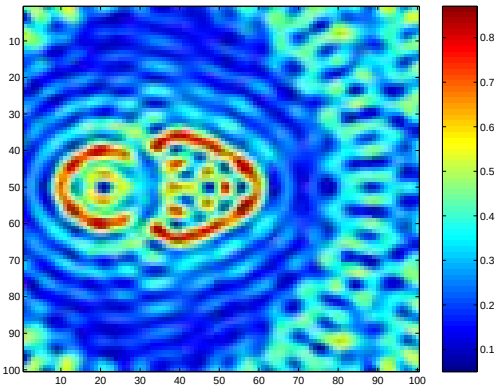

Figure 10: MUSIC imaging function with $k = 5$ for two sound-soft targets(one kite and one circle) that are very close to each other.

[12] A. Kirsch. The music algorithm and the factorization method in inverse scattering theory for inhomogenious media. *Inverse Problems*, 18:1025–1040, 2002.

[13] R. Kress. On the numerical solution of a hypersingular integral equation in scattering theory. *Journal of Computational and Applied Mathematics*, 1995.

[14] Claire Prada and Jean-Louis Thomas. Experimental subwavelength localization of scatterers by decomposition of the time reversal operator interpreted as a covariance matrix. *Journal of the Acoustical Society of America*, 114(1):235–243, 2003.

[15] R. O. Schmidt. Multiple emitter location and signal parameter estimation. *IEEE Trans. Antennas Propagation.*, 34(3):276–280, 1986.

[16] H. Zhao. Analysis of the response matrix for an extended target. *SIAM Applied Mathematics*, 64 (3):725–745, 2004.